pH Dependence of a Mammalian Polyamine Oxidase: Insights into Substrate Specificity and the Role of Lysine 315[†]

Michelle Henderson Pozzi,[‡] Vijay Gawandi,[‡] and Paul F. Fitzpatrick*[,‡,§]

Departments of Biochemistry and Biophysics and of Chemistry, Texas A&M University, College Station, Texas 77843-2128

Received December 5, 2008; Revised Manuscript Received January 7, 2009

ABSTRACT: Mammalian polyamine oxidases (PAOs) catalyze the oxidation of N1-acetylspermine and N1-acetylspermidine to produce N-acetyl-3-aminopropanaldehyde and spermidine or putrescine. Structurally, PAO is a member of the monoamine oxidase family of flavoproteins. The effects of pH on the kinetic parameters of mouse PAO have been determined to provide insight into the protonation state of the polyamine required for catalysis and the roles of ionizable residues in the active site in amine oxidation. For N1-acetylspermine, N1-acetylspermidine, and spermine, the k_{cat}/K_{amine}−pH profiles are bell-shaped. In each case, the profile agrees with that expected if the productive form of the substrate has a single positively charged nitrogen. The pK_i−pH profiles for a series of polyamine analogues are most consistent with the nitrogen at the site of oxidation being neutral and one other nitrogen being positively charged in the reactive form of the substrate. With N1-acetylspermine as the substrate, the value of k_{red}, the limiting rate constant for flavin reduction, is pH-dependent, decreasing below a pK_a value of 7.3, again consistent with the requirement for an uncharged nitrogen for substrate oxidation. Lys315 in PAO corresponds to a conserved active site residue found throughout the monoamine oxidase family. Mutation of Lys315 to methionine has no effect on the k_{cat}/K_{amine} profile for spermine; the k_{red} value with N1-acetylspermine is only 1.8-fold lower in the mutant protein, and the pK_a in the k_{red}−pH profile with N1-acetylspermine shifts to 7.8. These results rule out Lys315 as a source of a pK_a in the k_{cat}/K_{amine} or k_{cat}/k_{red} profiles. They also establish that this residue does not play a critical role in amine oxidation by PAO.

The polyamines spermine and spermidine are essential for cell proliferation, with higher levels being found in rapidly growing cells (*1, 2*). This observation suggests that compounds which decrease the levels of polyamines in cells have potential as antineoplastic agents. Indeed, the polyamine biosynthetic pathway has been heavily studied with the goal of developing enzyme inhibitors (*2*−*4*). The pathway begins with the formation of putrescine from ornithine catalyzed by ornithine decarboxylase. Putrescine is then converted to spermine by two sequential reactions catalyzed by spermidine synthase, forming first spermidine and then spermine, using decarboxylated S-adenosylmethione as the propylamine donor in both steps. In the opposite direction, catabolism of spermine requires the sequential action of two enzymes (*1*). First, acetylation of spermine by spermidine/spermine N1-acetylspermine acetyltransferase forms N1-acetylspermine. This is then converted to spermidine by the flavoenzyme polyamine oxidase (PAO).[1] The same two enzymes also catalyze the acetylation of spermidine to N1-acetylspermidine and the subsequent oxidation to putrescine. Very recently, several mammalian tissues have been found to contain a flavoenzyme capable of oxidizing spermine directly to spermidine (*5*−*7*); while referred to occasionally as PAO, it is more accurately a spermine oxidase.

Scheme 1

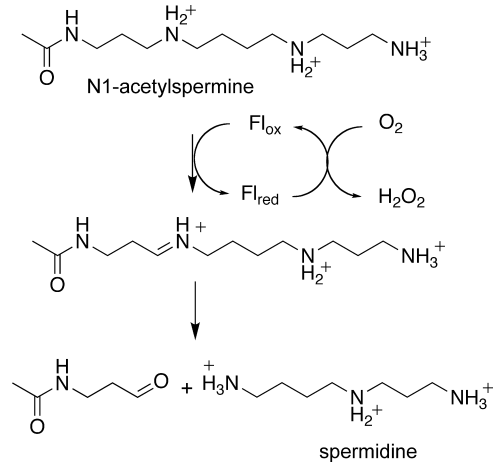

The reaction of mammalian PAO is shown in Scheme 1. The enzyme cleaves the *exo* carbon−hydrogen bond of its substrate, forming spermidine and N-acetyl-3-aminopropanaldehyde from N1-acetylspermine or putrescine and N-acetyl-3-aminopropanaldehyde from N1-acetylspermidine. There are also plant PAOs, of which the maize enzyme is the best-characterized (*8*−*11*). While the mammalian en-

[†] This work was supported in part by grants from the National Institutes of Health (R01 GM58698 to P.F.F. and T32 GM065088 to M.H.P.) and The Welch Foundation (A-1245 to P.F.F.).

* To whom correspondence should be addressed: Department of Biochemistry, MC 7760, University of Texas Health Science Center at San Antonio, San Antonio, TX 78229-3900. Phone: (210) 567-8264. Fax: (210) 567-8778. E-mail: fitzpatrickp@uthscsa.edu.

[‡] Department of Biochemistry and Biophysics.

[§] Department of Chemistry.

[1] Abbreviations: PAO, polyamine oxidase; MAO, monoamine oxidase; LSD1, lysine-specific histone demethylase 1; Fms1, *Saccharomyces cerevisiae* spermine oxidase; DAAO, D-amino acid oxidase.

10.1021/bi802227m CCC: $40.75
Published on Web 01/30/2009

zymes oxidize spermine to 3-aminopropanaldehyde and spermidine, the plant enzymes oxidize the *endo* bond of spermine to form propane-1,3-diamine and N-(3-aminopropyl)-4-aminobutyraldehyde (*12*). The structural bases for the difference in substrate specificity between polyamine and spermine oxidases and in the site of substrate oxidation between the plant and animal enzymes are not known.

The general reaction of flavin amine oxidases such as PAO can be divided into two half-reactions. In the reductive half-reaction, a hydride equivalent is transferred from the substrate to the flavin, while the oxidative half-reaction involves the oxidation of the reduced flavin by molecular oxygen, producing H_2O_2. The steady-state kinetic mechanism has previously been determined for mouse PAO (*13*). Consistent with the results for most flavoprotein oxidases (*14*), the kinetic pattern is ping-pong due to the reductive half-reaction being effectively irreversible. Consequently, the k_{cat}/K_m value for the amine substrate includes the steps in the reductive half-reaction from amine binding through flavin reduction, while the k_{cat}/K_m value for oxygen is the second-order rate constant for reoxidation of the reduced flavin. This simplifies analysis of the individual kinetic parameters, since the k_{cat}/K_m value for the amine substrate is independent of the oxygen concentration, while the rate constant for flavin reduction can readily be determined using rapid-reaction methods in the absence of oxygen.

The chemical mechanism of the reductive half-reaction of flavoprotein amine oxidases has been quite controversial (*15*). Oxidation of an amine substrate by an amine oxidase necessarily involves the removal of two protons and two electrons as the carbon−nitrogen single bond is converted to a double bond. The various mechanistic proposals for the flavin amine oxidases have included most of the possible combinations by which this can occur (*15, 16*). Cleavage of the carbon−hydrogen bond could occur by removal of the hydrogen as a proton, a hydrogen atom, or a hydride (*17*−*19*), with some mechanisms involving formation of an amine−flavin adduct as an intermediate (*19*). In contrast, the hydrogen is generally proposed to be removed from the nitrogen as a proton, with the disagreement over when this occurs in the reaction. Thus, the proton could be lost to solvent before the amine binds to the protein (*20*) or to an active site base either before (*21*−*23*) or concurrent with cleavage of the carbon−hydrogen bond (*21*). Thus, establishing the catalytic mechanism of an amine oxidase necessarily requires knowledge of the timing of removal of hydrogens from both the carbon and the nitrogen. In addition, in the case of the proton on the nitrogen, loss of the proton from the bound substrate would require an active site base.

The flavin amine oxidases can be divided into two structural classes, the monoamine oxidase (MAO) family (*9, 24*) and the D-amino acid oxidase (DAAO) family (*25*). No structure of a mammalian PAO has been described to date. However, structures are available for maize PAO and for *Saccharomyces cerevisiae* spermine oxidase (Fms1) (*26, 27*). These enzymes both belong to the MAO family (*26*). The sequences of mammalian PAOs align well with those of these and other members of this family (*13, 26, 28*). The available structures of members of the MAO family show that all contain a conserved lysyl residue in the active site (*24, 26*−*30*). This residue is part of a "Lys-H_2O-N5" motif in which the lysyl side chain forms hydrogen bonds to N5 of the isoalloxazine ring via an intervening water molecule. This lysyl residue has been proposed to be an active site base which accepts a proton from either the protonated amine of the substrate prior to its oxidation or a water molecule to form hydroxide for hydrolysis of an imine intermediate (*8, 24*).

This paper describes the use of the effects of pH on the steady-state and reductive half-reaction kinetics of mouse PAO to probe substrate specificity and establish the protonation states of polyamines required for catalysis. In addition, the role the conserved lysyl residue plays in amine oxidation by this enzyme has been analyzed.

EXPERIMENTAL PROCEDURES

Materials. Spermine was purchased from Acros Organics (Geel, Belgium), and 1,8-diaminooctane and 1,12-diaminododecane were purchased from Aldrich (Milwaukee, WI). N1-Acetylspermine and N1-acetylspermidine were synthesized as previously described (*31*); N1-acetylspermidine was also purchased from Fluka.

Syntheses. (i) N1-Acetyl-1,8-diaminododecane Hydrochloride. 1,8-Diaminooctane (3.5 mmol, 0.5 g) was added to 45 mL of ice-cold glacial acetic acid with magnetic stirring. The mixture was then heated to 55−60 °C. A solution of 0.33 mL of acetic anhydride (1.0 equiv) in 10 mL of glacial acetic acid was added dropwise with stirring over 1 h. The mixture was cooled to 25 °C and left overnight at that temperature. The residue after evaporation of the solvent under reduced pressure was dissolved in hot water, cooled, and adjusted to acidic pH with 6 N HCl. The solvent was removed, and the remaining solid was extracted twice with 50 mL of 2-propanol; any insoluble material was discarded. The combined filtrates were concentrated and cooled to −10 °C. The crystals that formed were collected by filtration and recrystallized from 75 mL of hot 2-propanol. The yield was 0.21 g (32%): ^{1}H NMR ($CDCl_3$) δ 6.41 (1H, s), 2.79 (2H, t), 2.57 (2H, t), 1.98 (3H, s), 1.58 (2H, m), 1.37 (8H, t), 1.46 (2H, m), 1.09 (2H, s); HRMS (m + H) theoretical 187.19, found 187.22.

(ii) N1-Acetyl-1,12-diaminododecane Hydrochloride. N1-Acetyl-1,12-diaminododecane hydrochloride was synthesized by a similar procedure from 1,12-diaminododecane. The yield was 0.18 g (∼31%): ^{1}H NMR ($CDCl_3$) δ 6.38 (1H, s), 2.74 (2H, t), 2.65 (2H, t), 1.95 (3H, s), 1.52 (2H, m), 1.38 (18H, m), 1.11 (1H, s); HRMS (m + H) theoretical 243.211, found 243.209.

(iii) N1-Acetyl-N3-pentyl-1,3-diaminopropane. To 3-aminopropanol (1.0 g, 13 mmol) in 5 mL of dry acetonitrile was added dropwise 1 equiv (2.9 g, 13 mmol) of $(Boc)_2O$ in 1.0 equiv (1.85 mL, 13 mmol) of triethylamine. After 6 h at 25 °C, an additional 0.5 equiv (1.4 g) of $(Boc)_2O$ was added. The reaction was continued overnight until silica gel thin-layer chromatography in a hexane/ethyl acetate mixture (8:2) showed one major spot. The solvent was evaporated in vacuo. The brown residue was treated with 1 M $KHSO_4$ (60 mL) and ether (100 mL). The solution was extracted with ether (4 × 25 mL), and the combined organic layers were washed with 50 mL each of 1 M $KHSO_4$ and 1 M $NaHCO_3$ and twice with a saturated solution of NaCl. The yellowish extract was dried ($MgSO_4$) and the solvent removed under vacuum. The brown residue was chromato-

graphed on silica using a hexane/ethyl acetate mixture (8:2) to give 1.25 g (54%) of N-Boc-3-aminopropanol: ^{1}H NMR ($CDCl_3$) δ 7.38 (1H, s), 3.72 (2H, m), 1.71 (2H, m), 2.55 (2H, t), 1.32 (9H, s).

The Boc-protected aminopropanol (1.0 g, 5.7 mmol) was added to 1.0 equiv (0.65 g, 5.7 mmol) of methanesulfonyl chloride in 2 mL of anhydrous pyridine. After 2 h at 25 °C, the reaction mixture was treated with 1 M $NaHCO_3$ (30 mL) and ether (70 mL). The solution was extracted with ether (3 × 25 mL), and the combined organic layers were washed with a saturated NaCl solution (2 × 50 mL). A brownish crude product was obtained after evaporation of solvent. Silica gel column chromatography using a hexane/ethyl acetate mixture (8:2) as the solvent yielded 0.75 g (52%) of N-Boc-3-amino-1-methanesulfonoxypropane: ^{1}H NMR ($CDCl_3$) δ 2.35 (3H, s), 4.21 (2H, t), 1.72 (2H, m), 2.81 (2H, t), 1.35 (9H, s).

N-Boc-3-amino-1-methanesulfonoxypropane (0.5 g, 2.0 mmol) was added to 1.0 equiv (0.17 g, 2.0 mmol) of 1-aminopentane in 5 mL of dry dichloromethane. After 5 h at 50 °C, the reaction mixture was cooled, washed with saturated Na_2CO_3, and extracted with ether. Silica gel chromatography using a hexane/ethyl acetate mixture (9:1) as the solvent gave 0.32 g (67%) of N-(N-Boc-3′-aminopropyl)-1-aminopentane: ^{1}H NMR ($CDCl_3$) δ 7.43 (1H, s), 2.71 (4H, m), 2.51 (2H, m), 1.73 (4H, m), 1.40 (4H, m), 1.33 (9H, s), 1.21 (3H, m), 1.12 (1H, s).

N-(N-Boc-3′-aminopropyl)-1-aminopentane (0.325 g, 1.33 mmol) in dioxane (5 mL) was treated with 10 mL of 4 M HCl with stirring at 25 °C for 5 h. After evaporation of the solvent under reduced pressure, the sticky residue was dissolved in distilled water (50 mL) and extracted with ether (3 × 20 mL). The aqueous layer was then passed through a C18 reverse phase column. The compound was eluted with a 20% ethanol/water mixture. Fractions were collected, flushed with N_2, and lyophilized to afford 115 mg (60%) of N-(3′-aminopropyl)-1-aminopentane: ^{1}H NMR (D_2O) δ 2.65 (6H, t), 1.67 (4H, m), 1.55 (4H, m), 1.28 (3H, s).

N-(3′-Aminopropyl)-1-aminopentane (0.115 g, 0.8 mmol) was added to 15 mL of cooled glacial acetic acid with stirring. The mixture was then heated to 55−60 °C. A mixture of 0.1 mL of acetic anhydride (1.05 equiv) in 2 mL of glacial acetic acid was added with stirring over a 1 h period. The solution was stored at 25 °C overnight and then evaporated to dryness. The residue was dissolved in hot water, cooled, and adjusted to acidic pH with 6 N HCl. After evaporation to dryness in vacuo, the resulting solid was extracted twice with 20 mL of 2-propanol, and the insoluble residue was discarded. The combined filtrates were concentrated and cooled to −10 °C. The crystals that formed were collected by filtration and recrystallized from 30 mL of hot 2-propanol. The yield of N1-acetyl-N3-pentyl-1,3-diaminopropane was 50 mg (34%): ^{1}H NMR ($CDCl_3$) δ 6.38 (1H, s), 2.68 (4H, m), 2.49 (2H, m), 1.97 (3H, s), 1.75 (2H, m), 1.72 (2H, m), 1.44 (4H, m), 1.23 (3H, m), 1.15 (1H, s); HRMS (m + H) theoretical 187.121, found 187.102.

Expression and Purification of Recombinant Proteins. Mouse PAO was purified as previously described (*32*) with a few minor changes. The pellet resulting from the final 65% ammonium sulfate precipitation was resuspended in 50 mM potassium phosphate and 10% glycerol (pH 7.5) and dialyzed overnight with two buffer changes. The resulting protein sample was then centrifuged at 22400*g* for 30 min at 4 °C to remove precipitated protein. The purified protein was stored at −80 °C. The concentration of active enzyme was determined from the flavin visible absorbance spectrum, using an ε_{458} value of 10400 M^{-1} cm^{-1}.

The K315M mutation was introduced using the Stratagene QuikChange site-directed mutagenesis method and mutagenic primer 5′-GGCTTCGGTACCAACAAC**ATG**ATCTTCCTC-GAGTTC-3′, which contains the K315M mutation (shown in bold) and a silent mutation at Leu318 that results in the addition of an *Ava*I site (underlined) used in screening colonies. The DNA sequence of the entire gene was carried out to ensure that no unwanted mutations occurred. Purification of the mutant enzyme was conducted using the same procedure that was used for wild-type PAO.

Assays. Steady-state kinetic assays were performed in air-saturated buffers on a computer-interfaced Hansatech (Hansatech Instruments) or YSI (Yellow Springs Instrument, Inc.) oxygen electrode. Assays were initiated by the addition of enzyme. All buffers contained 10% glycerol; 50 mM Tris-HCl, 50 mM CHES, and 50 mM CAPS were used for the pH ranges of 7−8.5, 9.0−9.5, and 10−11, respectively.

Rapid-reaction kinetic experiments were conducted at 20 °C on an Applied Photophysics SX-18MV stopped-flow spectrophotometer. The night before the experiment, the instrument was flushed with anaerobic buffer followed by a solution of 36 nM glucose oxidase in 5 mM glucose and 50 mM Tris-HCl (pH 7.5). For enzyme solutions, anaerobic conditions were established by applying cycles of vacuum and argon, while substrate solutions were bubbled with argon. All buffers contained 10% glycerol and 5 mM glucose; 200 mM PIPES, 200 mM Tris-HCl, and 200 mM CHES were used for the pH ranges of 6.5−6.9, 7−8.9, and 9.0−9.5, respectively. Glucose oxidase was added to all anaerobic solutions at a final concentration of 36 nM before they were loaded onto the stopped-flow spectrophotometer.

Data Analysis. Kinetic data were analyzed using KaleidaGraph (Adelbeck Software, Reading, PA) and Igor (WaveMetrics, Lake Oswego, OR). Initial rate data obtained by varying the concentration of a single substrate were fit to the Michaelis−Menten equation. The effects of pH on kinetic parameters were fit to eqs 1−3. Equation 1 applies for a kinetic parameter which decreases below pK_1 due to the protonation of a single moiety. Equation 2 applies for a kinetic parameter which decreases above pK_2 due to the protonation of a single moiety. Equation 3 applies for a kinetic parameter which decreases below pK_1 due to protonation of a singe moiety and decreases above pK_2 due to deprotonation of a single moiety. In each, y is the kinetic parameter being measured, c is the pH-independent value, K_1 is the ionization constant for a residue which must be unprotonated, and K_2 is the ionization constant for a residue which must be protonated.

$$\log y = \log[c/(1 + H/K_1)] \quad (1)$$

$$\log y = \log[c/(1 + K_2/H)] \quad (2)$$

$$\log y = \log[c/(1 + H/K_1 + K_2/H)] \quad (3)$$

Analysis of stopped-flow data was carried out using both KaleidaGraph and SPECFIT (Spectrum Software Associates, Marlborogh, MA). To determine the kinetic parameters for the reduction of wild-type PAO by N1-acetylspermine,

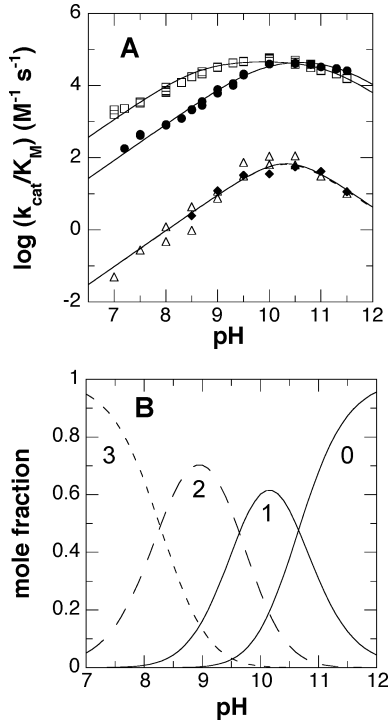

FIGURE 1: (A) k_{cat}/K_{amine}−pH profile of wild-type PAO with N1-acetylspermine (□), N1-acetylspermidine (●), and spermine (△) and K315M PAO with spermine (◆). The lines are from fits of the data to eq 3. (B) Theoretical protonation states of N1-acetylspermine with no proton, one proton, two protons, or three protons.

stopped-flow traces were fit to eq 4, which describes a triphasic exponential decay, where k_1, k_2, and k_3 are first-order rate constants, A_1, A_2, and A_3 correspond to the absorbance changes in each phase, and A_∞ is the final absorbance. Equation 5 was used to fit the biphasic traces obtained for K315M PAO.

$$A_t = A_1 e^{-k_1 t} + A_2 e^{-k_2 t} + A_3 e^{-k_3 t} + A_\infty \quad (4)$$

$$A_t = A_1 e^{-k_1 t} + A_2 e^{-k_2 t} + A_\infty \quad (5)$$

Calculation of Polyamine Protonation States. The microscopic pK_a values for each of the nitrogens in N1-acetylspermine, N1-acetylspermidine, spermidine, and spermine were calculated using the method of Aikens et al. (*33*) and the values of Clark and Perrin (*34*). These values were then used to calculate the mole fractions with zero, one, two, three, or four charged nitrogens as a function of pH. A value of 0.15 was subtracted from each pK_a value to correct for the difference between 25 and 30 °C.

RESULTS

k_{cat}/K_{amine}−pH Profile. Previous steady-state kinetic studies at pH 7.6 indicated that the substrate preference for mouse PAO is N1-acetylspermine, N1-acetylspermidine, and then spermine, with spermine being a significantly slower substrate than the acetylated compounds (*13*). The effect of pH on the kinetic parameter k_{cat}/K_{amine} was determined for each of these three substrates. The results are shown in Figure 1A, and the resulting pK_a values are summarized in Table 1. The pH profiles for all three substrates exhibit decreases in activity at both low and high pH, consistent with a requirement for one moiety in the enzyme or substrate that must be protonated for substrate recognition and/or oxidation and one which must be unprotonated.[2] Both acetylated substrates have bell-shaped curves with two distinguishable pK_a values. In contrast, with spermine the pH profile exhibits a sharp optimum so that the two pK_a values are too close together to resolve; consequently, only the average of the two pK_a values could be determined with this substrate.

Table 1: pK_a Values for PAO Substrates and Inhibitors

kinetic parameter	pK_{a1}	pK_{a2}
wild-type PAO		
k_{cat}/K_m for N1-acetylspermine	8.5 ± 0.1	11.2 ± 0.1
k_{cat}/K_m for N1-acetylspermidine	9.8 ± 0.1	11.3 ± 0.3
k_{cat}/K_m for spermine	10.3 ± 0.1	10.3 ± 0.1
K_i for N1-acetyl-1,8-diaminooctane	−	11.6 ± 0.1
K_i for 1,8-diaminooctane	9.3 ± 0.1	10.8 ± 0.1
K_i for N1-acetyl-N3-pentyl-1,3-diaminopropane	8.9 ± 0.1	−
K_i for 1,12-diaminododecane	10.0 ± 0.1	10.0 ± 0.1
K_i for N1-acetyl-1,12-diaminododecane	−	11.6 ± 0.1
K315M PAO		
k_{cat}/K_m for spermine	10.3 ± 0.1	10.3 ± 0.1

Protonation States of Polyamines as a Function of pH. A likely basis for one or both of the pK_a values in the k_{cat}/K_{amine}−pH profiles is the protonation state of the substrates. A number of authors have determined the macroscopic pK_a values for spermine (*35*−*39*), but we have been unable to find experimental values for N1-acetylspermine and N1-acetylspermidine. However, even the pK_a values for spermine reflect protonations at multiple sites, in that the intrinsic pK_a values of the individual nitrogens are not very different. Binding in the active site of PAO is likely instead to require that each nitrogen be either fully protonated or fully unprotonated. Consequently, the microscopic pK_a values for each nitrogen were calculated for spermine, spermidine, N1-acetylspermine, and N1-acetylspermidine (Table S1 of the Supporting Information). To determine the reliability of these pK_a values, they were used to calculate the macroscopic pK_a values for spermine and spermidine; in both cases, the values for all the nitrogens were consistent with published values (Table S2 of the Supporting Information). The calculated microscopic pK_a values were then used to determine the effect of pH on the mole fraction of each polyamine with an integral number of protons. Figure 1B shows the effect of pH on the mole fractions of N1-acetylspermine with zero, one, two, or three protons. The monoprotonated form is maximal at pH 10.1, in good agreement with the pH optimum in the k_{cat}/K_{amine}−pH profile of 9.9, while the diprotonated form is maximal at pH 9.0. For spermine, the pH maximum for the monoprotonated form is 10.4−10.5 (Table S2 and Figure S1 of the Supporting Information and refs *35* and *38*), similarly closer to the pH optima of 10.3 than is the maximum for the diprotonated form of 9.4−9.5. The agreement with N1-acetylspermidine is not as good, in that the optimum in the k_{cat}/K_{amine}−pH profile is 10.5 while the calculated maximum for the monoprotonated form is 9.9

[2] The presence of three or four nitrogen atoms in N1-acetylspermine and spermine which have pK_a values in the accessible range should yield pH profiles more complex than simple bell shapes, with slopes of ±2 at pH values where additional nitrogens are incorrectly protonated. However, no improvement in the data fitting was seen when an additional pK_a was incorporated into the equation. Simulations of the effect of the additional nitrogen(s) showed that the effect was negligible over the pH range used here.

Scheme 2

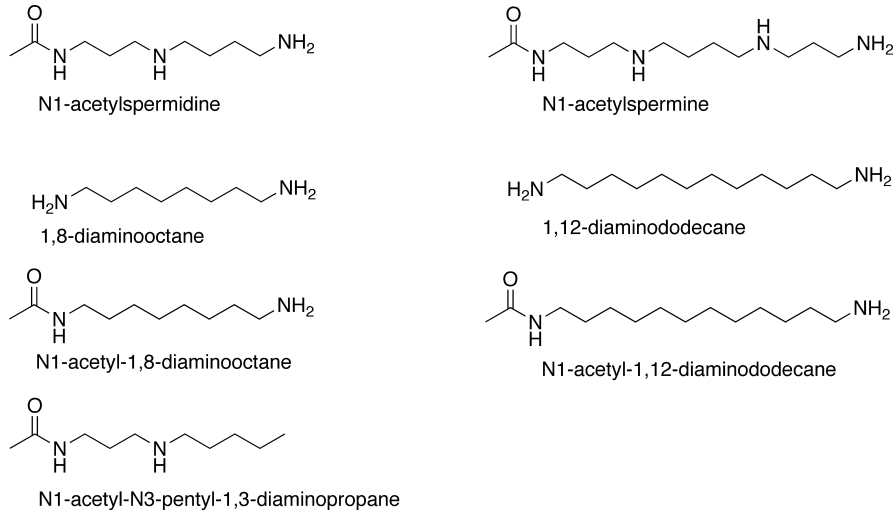

(Figure S1 of the Supporting Information). However, a requirement for the diprotonated form of N1-acetylspermidine would contribute a single pK_a of 9.1 for a group which must be protonated to the k_{cat}/K_{amine}−pH profile, while a requirement for the uncharged form would contribute a single pK_a value of 10.6 (Table S2 and Figure S1 of the Supporting Information), in contrast to the observed bell-shaped profile. Thus, the k_{cat}/K_{amine}−pH profiles are most consistent with the active form of the substrate having a single charge.

PAO pH Dependence of Inhibition. While the k_{cat}/K_{amine}−pH profiles are consistent with the monoprotonated forms of the substrate being preferred, they do not establish which nitrogen in each substrate must be charged. In addition, the k_{cat}/K_{amine}−pH profiles reflect both binding and catalysis. To determine the preferred protonation states of individual nitrogens in substrates for productive binding, analogues lacking one or more nitrogens (Scheme 2) were characterized as inhibitors. 1,8-Diaminooctane, N1-acetyl-1,8-diaminooctane, and N1-acetyl-N3-pentyl-1,3-diaminopropane all mimic the substrate N1-acetylspermidine. Each is a competitive inhibitor versus the amine (data not shown). The pK_i−pH profile for 1,8-diaminooctane is bell-shaped with the tightest binding at pH 10 (Figure 2A and Table 1), consistent with binding requiring that one nitrogen on the inhibitor be protonated and one be unprotonated. With N1-acetyl-1,8-diaminooctane, the only protonatable group is the amino group on carbon 8; in this case, the pK_i−pH profile shows a decrease at high pH with a pK_a value of 11.6 ± 0.1, but no decrease at low pH (Figure 2A). This is most consistent with the acidic pK_a in the pH profile for N1-acetylspermine being due to a need for N9 to be charged. N1-Acetyl-N3-pentyl-1,3-diaminopropane also has only one protonatable nitrogen group, located at the 4 position, the site of oxidation in N1-acetylspermidine. In this case, the pK_i−pH profile shows a decrease at low pH with a pK_a value of 8.9 ± 0.1, but no decrease at high pH, indicating that N4 must be unprotonated. These results are consistent with the active form of N1-acetylspermidine being the monoprotonated species in which N9 is protonated and N4 is unprotonated.

Similar studies were conducted with analogues of N1-acetylspermine and spermine. 1,12-Diaminododecane shows a bell-shaped pK_i−pH profile with an average pK_a value of 10.0 ± 0.1 (Figure 2B). This matches well the k_{cat}/K_{amine}−pH profile for spermine (Table 1), consistent with productive binding requiring a substrate with a single positive charge. The pK_i−H profile for the N1-acetylspermine analogue N1-acetyl-1,12-diaminododecane shows a decrease at high pH with a single pK_a value of 11.6 ± 0.1 (Figure 2B), confirming that a nitrogen not located next to the site of C−H bond cleavage must be protonated for catalysis.

pH Dependence of Flavin Reduction. To address the effect of pH on catalysis rather than binding, stopped-flow spectroscopy was used to determine the rate constant for flavin reduction by N1-acetylspermine as a function of pH. Reac-

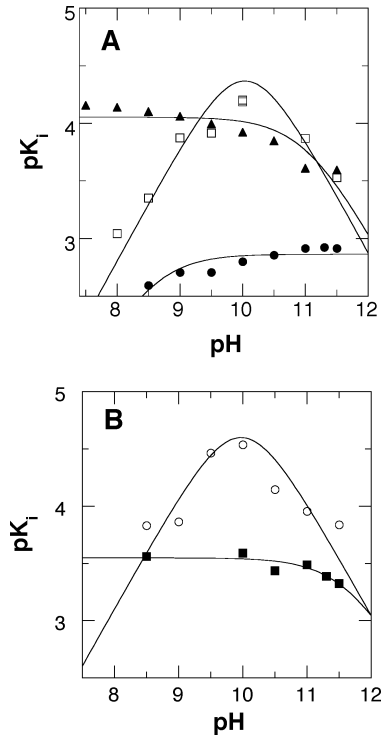

FIGURE 2: pK_i−pH profile of wild-type PAO with (A) N1-acetyl-N3-pentyl-1,3-diaminopropane (●), 1,8-diaminooctane (□), and N1-acetyl-1,8-diaminooctane (▲) and (B) N1-acetyl-1,12-diaminododecane (■) and 1,12-diaminododecane (○). The lines are from fits to eq 1 for N1-acetyl-N3-pentyl-1,3-diaminopropane, to eq 2 for N1-acetyl-1,8-diaminooctane and N1-acetyl-1,12-diaminododecane, and to eq 3 for 1,8-diaminooctane and 1,12-diaminododecane.

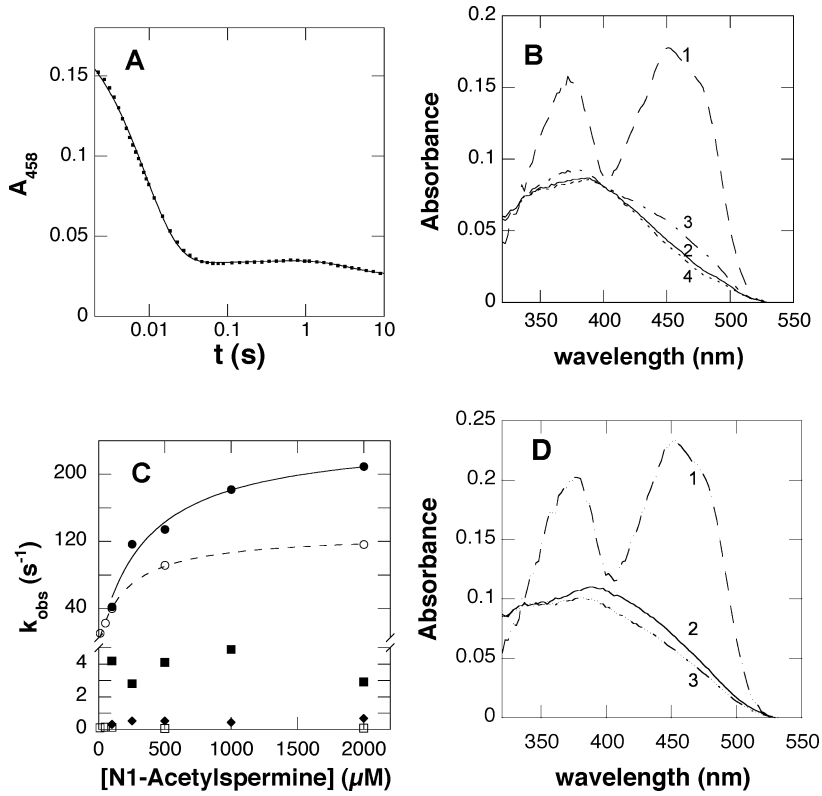

FIGURE 3: Reduction of PAO by 1 mM N1-acetylspermine at pH 7.5 and 20 °C. (A) Absorbance changes at 458 nm upon reduction of 20 μM wild-type PAO by 1 mM N1-acetylspermine. The line is from a fit to eq 4. (B) Absorbance spectra of flavin intermediates observed in the reductive half-reaction of wild-type PAO. (C) Dependence of the individual rate constants on the N1-acetylspermine concentration for wild-type [first phase (●), second phase (■), and third phase (◆)] and K315M [first phase (○) and second phase (□)] PAO. The lines are from fits of the concentration dependence of the rate constant for the first phase to the Michaelis−Menten equation. (D) Absorbance spectra of the flavin intermediates observed in the reductive half-reaction of K315M PAO.

tions were carried out at 20 °C instead of 30 °C because much of the reaction occurred in the dead time of the instrument at the higher temperature. Over the pH range of 6.5−9.5, the flavin absorbance at 458 nm showed the same behavior: an initial decrease in absorbance, a slower, slight increase in absorbance, and finally a slow decrease in absorbance (Figure 3A). Data could not be obtained at pH 10 and above due to enzyme instability. The same kinetic behavior was seen when the reaction was monitored from 320 to 600 nm by photodiode array spectroscopy; this approach also allowed the spectra of the intermediates to be obtained (Figure 3B). The initial fast phase of the reaction accounts for the majority of the change in amplitude and has a rate constant that is dependent on substrate concentration (Figure 3C). This phase can be attributed to the rapid and reversible binding of N1-acetylspermine with no detectable change in the flavin spectrum, followed by flavin reduction. The slowest two rate constants are independent of substrate concentration and slower than k_{cat} (Figure 3C); therefore, they are not relevant to catalysis.

The effect of pH on the rate constant for reduction of PAO at saturating concentrations of N1-acetylspermine (k_{red}) is shown in Figure 4. The value of this kinetic parameter shows a decrease at acidic pH with a pK_a of 7.3 ± 0.1, indicating that a group in the ES complex must be unprotonated for reduction. Flavin reduction is significantly faster than k_{cat} over the pH range investigated, so that the oxidative half-reaction is rate-limiting for turnover with this substrate.

K315M PAO. Figure 5 shows the relative positions of the FAD and the conserved active site lysine in the structures

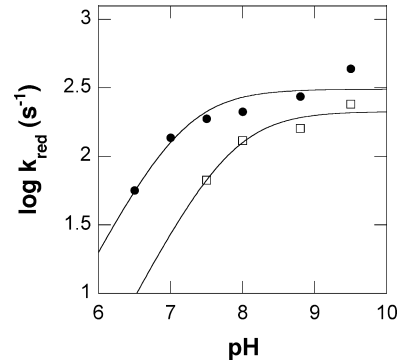

FIGURE 4: pH dependence of k_{red} for wild-type (●) and K315M (□) PAO with N1-acetylspermine at 20 °C. The lines are from fits of the data to eq 1.

of several members of the MAO structural family. On the basis of sequence alignment, PAO Lys315 corresponds to this conserved residue. The location of this lysine with respect to the flavin makes it a potential source of a pK_a in the k_{cat}/K_{amine}− and k_{red}−pH profiles. Consequently, the K315M mutation was introduced into PAO. The circular dichroism spectrum of the mutant protein did not reveal any significant changes compared to wild-type PAO, suggesting the K315M mutation does not affect the overall folding of the protein or the flavin environment (data not shown). The K_M value for N1-acetylspermine is less than 10 μM for the mutant protein (data not shown), so the k_{cat}/K_{amine}−pH profile for this mutant was only determined using the substrate spermine. The $k_{cat}/K_{spermine}$ value for K315M PAO is identical to that for wild-type PAO over the entire pH range (Figure

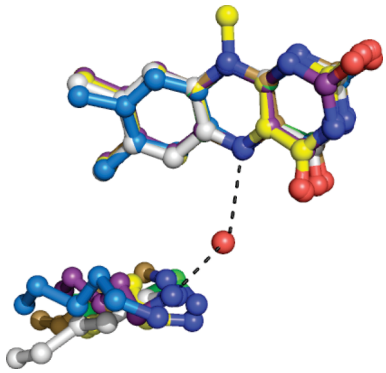

FIGURE 5: Relative positions of the conserved active site lysine and the FAD in human MAO A (blue carbons), human MAO B (purple carbons), maize PAO (yellow carbons), *S. cerevisiae* spermine oxidase Fms1 (green carbons), *Calloselasma rhodostoma* L-amino acid oxidase (gray carbons), and human LSD1 (light brown carbons). This figure was composed from PDB entries 2BXS (MAO A), 1OJ9 (MAO B), 1H83 (maize PAO), 1RSG (Fms1), 1F8S (L-amino acid oxidase), and 2HKO (LSD1). To generate this figure, the atoms of the central pyrazine rings of the FAD cofactors were overlaid. The water molecule shown is from maize PAO.

1A and Table 1), resulting in an identical pK_a of 10.3. Thus, Lys315 is not critical for polyamine oxidation, and ionization of Lys315 does not contribute to the k_{cat}/K_{amine}−pH profile.

To further investigate the role of Lys315 in catalysis, the effect of pH on the value of k_{red} with N1-acetylspermine was determined for the mutant protein. The changes in the flavin spectrum upon reduction of K315M PAO are biphasic, with a fast phase exhibiting a large change in absorbance and a slower phase exhibiting a smaller amplitude (Figure 3C). As with the wild-type enzyme, the rate constant for the fast phase shows a dependence on substrate concentration, while the rate constant for the slow phase is independent of substrate concentration and is slower than the k_{cat} value for the mutant protein (Figure 3D). At pH 9.5, the value of k_{red} is not decreased substantially from the value for the wild-type enzyme (240 s^{-1} vs 440 s^{-1}), indicating that this mutation does not have a significant effect on the reductive half-reaction. The k_{red}−pH profile for K315M PAO is similar to that observed for the wild-type enzyme, with a basic shift in the pK_a to 7.8 ± 0.1 (Figure 4).

DISCUSSION

The protonation state of the amine substrate required for productive binding has been a subject of controversy among those studying flavin amine oxidases. For the DAAO family, Harris et al. (*21*) proposed that a coupled deprotonation/dehydrogenation of the protonated substrate occurs in which a proton is transferred to the solvent from DAAO. However, Denu and Fitzpatrick (*40*) reported that DAAO does not show a solvent isotope effect, leading to the conclusion that the amino group of the substrate must be uncharged. Further evidence for the amine being in the neutral form was provided by measurement of ^{15}N isotope effects for DAAO, which indicated that the amino group must be unprotonated for catalysis (*20*). Zhao and Jorns (*41*) subsequently concluded from studies of monomeric sarcosine oxidase that the amine substrate within the enzyme−substrate complex must be unprotonated for flavin reduction. The situation with the MAO/PAO family has been less clear. Jones et al. (*23*) concluded that uncharged inhibitors bind MAO A better, but the predominant species of the amine in the pH range of 7−9 is protonated and therefore must be the substrate. In contrast, Dunn et al. (*42*) concluded from kinetic isotope and pH studies with MAO A that deprotonation of the amine is required for catalysis. The studies reported here clearly show that mammalian PAO requires that N4 next to the site of C−H bond cleavage be unprotonated for C−H bond cleavage to occur. This is consistent with the results of Dunn et al. (*42*) with MAO, establishing that the enzymes of the MAO/PAO family all require an unprotonated nitrogen for amine oxidation, as do the members of the DAAO/sarcosine oxidase family. This requirement for a substrate with a neutral nitrogen extends the mechanistic similarities of these two structural classes of flavin amine oxidases, a clear example of convergent evolution of enzyme mechanisms.

Comparison of the effect of pH on the protonation state of each substrate with its k_{cat}/K_{amine}−pH profiles establishes that the monoprotonated forms are required for catalysis. More specifically, the pK_i−pH profiles for the inhibitors establish that these pK_as can be attributed to specific nitrogens in the substrates. In N1-acetylspermidine, the nitrogen next to the carbon being oxidized must be unprotonated and N10 must be protonated. N1-Acetylspermine and spermine are more complicated due to the increased number of nitrogens. For N1-acetylspermine, N4 must be unprotonated, but the data for the inhibitors do not establish whether it is N10 or N14 that must be protonated. However, the k_{cat}/K_{amine} values for N-acetylspermine and N1-acetylspermidine are identical at the pH optimum, suggesting that it is N10 that is protonated, as is the case for N1-acetylspermidine. A similar case can be made for spermine. These results suggest that both protonated and unprotonated forms of the substrate can bind, but only the protonated form can react. Thus, the pK_as in the k_{cat}/K_{amine}−pH profiles are due to the substrate and not an ionizable residue within the active site of the enzyme.

The requirement for the monoprotonated substrate provides a potential mechanism of discrimination against spermine by PAO, since an acetyl moiety would prevent the terminal nitrogen from ionizing and thereby result in a very large increase in the fraction of substrate in the correctly protonated form. Although the k_{cat}/K_{amine} values are essentially identical at pH 10 for the two natural substrates N1-acetylspermine and N1-acetylspermidine, at the physiological pH of approximately 8.2 (*43*), N1-acetylspermine is the far better substrate. Compared with N1-acetylspermidine, N1-acetylspermine has a broader pH profile (Figure 1A). This is most readily explained by a difference in the forward commitments of the two substrates, with N1-acetylspermine being a more sticky substrate.

The k_{red}−pH profile for wild-type PAO shows a pK_a of 7.3 with N1-acetylspermine as the substrate. The pH profile for k_{red} reports on the protonation states of ionizable groups in the enzyme−substrate complex required for reduction. The decrease in activity at acidic pH can be attributed to the substrate bound to the enzyme. The incorrectly protonated form of the substrate must be able to bind but not to react. If one assumes that substrate binding is at equilibrium, a likely oversimplification, the difference between the pK_a of the reactive nitrogen when bound to the enzyme and free in solution of 2.1 establishes that the correctly protonated form binds ~100-fold more tightly than the form with N4 protonated. Monomeric sarcosine oxidase and MAO A show

similar perturbations of the amine pK_a upon binding (*41, 42*), suggesting that the active sites of these enzymes also preferentially bind the form of the substrate with the critical nitrogen in its neutral form.

Although numerous mechanisms have been put forth for flavin amine oxidases, most recent data support the mechanism as direct hydride transfer. Kinetic studies using ^{15}N isotope effects have ruled out the possibility of a polar nucleophilic addition mechanism (*44, 45*). The ^{15}N isotope effects are consistent with a single-electron transfer mechanism, but the failure to detect any intermediate with a natural substrate for any flavin amine oxidase and the very unfavorable redox change for single electron transfer from an amine to an oxidized flavin provide arguments against such a mechanism. Reduction of wild-type PAO by N1-acetylspermine shows multiple phases, with the rate constant for the fastest phase reflecting amine oxidation, while the slower phases are likely due to the release of product from reduced enzyme, a step that is not significant during turnover in the presence of oxygen. More critically, the flavin spectrum showed no intermediate between fully oxidized and fully reduced flavin during reduction of wild-type PAO by N1-acetylspermine over the entire pH range studied, indicating that oxidation of the amine substrate to the imine occurs in a single step. This result is consistent with what has been observed with other flavin amine oxidases (*21, 46*−*48*).

The conserved active site lysyl residue in flavin amine oxidases provides a potential source of a pK_a in the k_{cat}/K_{amine} profile. The role of this residue has previously been examined in several members of this family. In maize PAO, when Lys300 is similarly mutated to a methionine, a 1400-fold decrease in k_{red} is observed, suggesting an important but undefined role for this residue in substrate oxidation (*8*). The corresponding K661A mutation in human LSD1 completely abolished demethylase activity (*49*). In contrast, the substitution of methionine for this lysine in PAO results in no change in the k_{cat}/K_{spm} value or the pH profile with spermine, and the rate constant for flavin reduction by N1-acetylspermine shows an only 1.8-fold decrease at pH 9.5. This rules out Lys315 acting as an active site base in mouse PAO or playing any other critical role in the reductive half-reaction. The k_{red}−pH profile for K315M PAO shows a slight basic shift in the pK_a as compared to that for wild-type PAO; this can be attributed to a change in the active site environment due to the loss of the charged lysine. The reasons for the differences in the effects of mutating this residue among the different flavin amine oxidases are not apparent. It may be that this residue plays a critical role in positioning the flavin or otherwise stabilizing the active site structure and that different flavin amine oxidases simply tolerate the loss of this interaction more than others.

In conclusion, this study establishes the protonation state of the amine required for productive binding to PAO, and presumably for the other members of the MAO/PAO family. The results will be of use in further studies of the mechanism of amine oxidation, for interpretation of the effects of site-directed mutagenesis, for design of inhibitors, and for understanding the different substrate specificities and reactivities of polyamine and spermine oxidases. The results rule out a critical role for Lys315 in polyamine oxidation and further support hydride transfer from the neutral amine as the mechanism of flavin amine oxidases.

SUPPORTING INFORMATION AVAILABLE

Comparison of calculated and measured macroscopic pK_a values for polyamines, calculated microscopic pK_a values used to calculate the macroscopic pK_a values and the mole fractions of the individual polyamines, and calculated mole fractions of the different protonated forms of spermine and N1-acetylspermidine. This material is available free of charge via the Internet at http://pubs.acs.org.

REFERENCES

1. Tabor, C. W., and Tabor, H. (1984) Polyamines. *Annu. Rev. Biochem. 53*, 749–790.
2. Marton, L. J., and Pegg, A. E. (1995) Polyamines as targets for therapeutic intervention. *Annu. Rev. Pharmacol. Toxicol. 35*, 55–91.
3. Lin, P. K. T., Dance, A. M., Bestwick, C., and Milne, L. (2003) The biological activities of new polyamine derivatives as potential therapeutic agents. *Biochem. Soc. Trans. 31*, 407–410.
4. Wang, Y., and Casero, R. A., Jr. (2006) Mammalian polyamine catabolism: A therapeutic target, a pathological problem, or both? *J. Biochem. 139*, 17–25.
5. Vujcic, S., Diegelman, P., Bacchi, C. J., Kramer, D. L., and Porter, C. W. (2002) Identification and characterization of a novel flavin-containing spermine oxidase of mammalian cell origin. *Biochem. J. 367*, 665–675.
6. Wang, Y., Murray-Stewart, T., Devereux, W., Hacker, A., Frydman, B., Woster, P. M., and Casero, R. A., Jr. (2003) Properties of purified recombinant human polyamine oxidase, PAOh1/SMO. *Biochem. Biophys. Res. Commun. 304*, 605–611.
7. Cervelli, M., Polticelli, F., Federico, R., and Mariottini, P. (2003) Heterologous expression and characterization of mouse spermine oxidase. *J. Biol. Chem. 278*, 5271–5276.
8. Polticelli, F., Basran, J., Faso, C., Cona, A., Minervini, G., Angelini, R., Federico, R., Scrutton, N. S., and Tavladoraki, P. (2005) Lys300 plays a major role in the catalytic mechanism of maize polyamine oxidase. *Biochemistry 44*, 16108–16120.
9. Binda, C., Mattevi, A., and Edmondson, D. E. (2002) Structure-function relationships in flavoenzyme dependent amine oxidations. A comparison of polyamine oxidase and monoamine oxidase. *J. Biol. Chem. 277*, 23973–23976.
10. Binda, C., Angelini, R., Federico, R., Ascenzi, P., and Mattevi, A. (2001) Structural bases for inhibitor binding and catalysis in polyamine oxidase. *Biochemistry 40*, 2766–2776.
11. Bellelli, A., Angelini, R., Laurenzi, M., and Federico, R. (1997) Transient kinetics of polyamine oxidase from *Zea mays* L. *Arch. Biochem. Biophys. 343*, 146–148.
12. Sebela, M., Radová, A., Angelini, R., Tavladoraki, P., Frébort, I., and Pec, P. (2001) FAD-containing polyamine oxidases: A timely challenge for researchers in biochemistry and physiology of plants. *Plant Sci. 160*, 197–207.
13. Wu, T., Yankovskaya, V., and McIntire, W. S. (2003) Cloning, sequencing, and heterologous expression of the murine peroxisomal flavoprotein, N1-acetylated polyamine oxidase. *J. Biol. Chem. 278*, 20514–20525.
14. Bright, H. J., and Porter, D. J. T. (1975) Flavoprotein oxidases. In *The Enzymes* (Boyer, P., Ed.) 3rd ed., Vol. XII, pp 421−505, Academic Press, New York.
15. Fitzpatrick, P. F. (2001) Substrate dehydrogenation by flavoproteins. *Acc. Chem. Res. 34*, 299–307.
16. Fitzpatrick, P. F. (2007) Insights into the mechanisms of flavoprotein oxidases from kinetic isotope effects. *J. Labelled Compd. Radiopharm. 50*, 1016–1025.
17. Scrutton, N. S. (2004) Chemical aspects of amine oxidation by flavoprotein enzymes. *Nat. Prod. Rep. 21*, 722–730.
18. Zhao, G., and Jorns, M. S. (2006) Spectral and kinetic characterization of the Michaelis charge transfer complex in monomeric sarcosine oxidase. *Biochemistry 45*, 5985–5992.
19. Edmondson, D. E., Binda, C., and Mattevi, A. (2007) Structural insights into the mechanism of amine oxidation by monoamine oxidases A and B. *Arch. Biochem. Biophys. 264*, 269–276.

20. Kurtz, K. A., Rishavy, M. A., Cleland, W. W., and Fitzpatrick, P. F. (2000) Nitrogen isotope effects as probes of the mechanism of D-amino acid oxidase. *J. Am. Chem. Soc. 122*, 12896–12897.
21. Harris, C. M., Pollegioni, L., and Ghisla, S. (2001) pH and kinetic isotope effects in D-amino acid oxidase catalysis: Evidence for a concerted mechanism in substrate dehydrogenation via hydride transfer. *Eur. J. Biochem. 268*, 5504–5520.
22. Zhao, G., Song, H., Chen, Z., Mathews, S., and Jorns, M. S. (2002) Monomeric sarcosine oxidase: Role of histidine 269 in catalysis. *Biochemistry 41*, 9751–9764.
23. Jones, T. Z., Balsa, D., Unzeta, M., and Ramsay, R. R. (2007) Variations in activity and inhibition with pH: The protonated amine is the substrate for monoamine oxidase, but uncharged inhibitors bind better. *J. Neural Transm. 114*, 707–712.
24. Pawelek, P. D., Cheah, J., Coulombe, R., Macheroux, P., Ghisla, S., and Vrielink, A. (2000) The structure of L-amino acid oxidase reveals the substrate trajectory into an enantiomerically conserved active site. *EMBO J. 19*, 4204–4215.
25. Trickey, P., Wagner, M. A., Jorns, M. S., and Mathews, F. S. (1999) Monomeric sarcosine oxidase: Structure of a covalently flavinylated amine oxidizing enzyme. *Structure 7*, 331–345.
26. Binda, C., Coda, A., Angelini, R., Federico, R., Ascenzi, P., and Mattevi, A. (1999) A 30 Å long U-shaped catalytic tunnel in the crystal structure of polyamine oxidase. *Structure 7*, 265–276.
27. Huang, Q., Liu, Q., and Hao, Q. (2005) Crystal structures of Fms1 and its complex with spermine reveal substrate specificity. *J. Mol. Biol. 348*, 951–959.
28. Binda, C., Newton-Vinson, P., Hubalek, F., Edmondson, D. E., and Mattevi, A. (2002) Structure of human monoamine oxidase B, a drug target for the treatment of neurological disorders. *Nat. Struct. Biol. 9*, 22–26.
29. Chen, Y., Yang, Y., Wang, F., Wan, K., Yamane, K., Zhang, Y., and Lei, M. (2006) Crystal structure of human histone lysine-specific demethylase 1 (LSD1). *Proc. Natl. Acad. Sci. U.S.A. 103*, 13956–13961.
30. Ma, J., Yoshimura, M., Yamashita, E., Nakagawa, A., Ito, A., and Tsukihara, T. (2004) Structure of rat monoamine oxidase A and its specific recognitions for substrates and inhibitors. *J. Mol. Biol. 338*, 103–114.
31. Gawandi, V., and Fitzpatrick, P. F. (2007) The synthesis of deuterium-labeled spermine, N1-acetylspermine and N1-acetylspermidine. *J. Labelled Compd. Radiopharm. 50*, 666–670.
32. Royo, M., and Fitzpatrick, P. F. (2005) Mechanistic studies of mouse polyamine oxidase with N1,N12-bisethylspermine as a substrate. *Biochemistry 44*, 7079–7084.
33. Aikens, D., Bunce, S., Onasch, F., Parker, R., III, Hurwitz, C., and Clemans, S. (1983) The interactions between nucleic acids and polyamines. II. Protonation constants and ^{13}C-NMR chemical shift assignments of spermidine, spermine, and homologs. *Biophys. Chem. 17*, 67–74.
34. Clark, J., and Perrin, D. D. (1964) Prediction of the strengths of organic bases. *Q. Rev. Chem. Soc. 18*, 295–320.
35. Frassineti, C., Ghelli, S., Gans, P., Sabatini, A., Moruzzi, M. S., and Vacca, A. (1995) Nuclear magnetic resonance as a tool for determining protonation constants of natural polyprotic bases in solution. *Anal. Biochem. 231*, 374–382.
36. Kimberly, M., and Goldstein, J. H. (1981) Determination of pK_a values and total proton distribution pattern of spermidine by carbon-13 nuclear magnetic resonance titrations. *Anal. Chem. 53*, 789–793.
37. Lomozik, L., Gasowska, A., and Bolewski, L. (1996) Copper(II) ions as a factor interfering in the interaction between bioligands in systems with adenosine and polyamines. *J. Inorg. Biochem. 63*, 191–206.
38. Bencini, A., Bianchi, A., Garcia-Espana, E., Micheloni, M., and Remirez, J. A. (1999) Proton coordination by polyamine compounds in aqueous solution. *Coord. Chem. Rev. 188*, 97–156.
39. da Silva, J. A., Felcman, J., Lopes, C. C., Lopes, R. S. C., and Villar, J. D. F. (2002) Study of the protonation/deprotonation sequence of two polyamines: Bis-[(2S)-2-pyrrolidinylmethyl] ethylenediamine and spermidine by ^{1}H and ^{13}C nuclear magnetic resonance. *Spectrosc. Lett. 35*, 643–661.
40. Denu, J. M., and Fitzpatrick, P. F. (1994) Intrinsic primary, secondary, and solvent kinetic isotope effects on the reductive half-reaction of D-amino acid oxidase: Evidence against a concerted mechanism. *Biochemistry 33*, 4001–4007.
41. Zhao, G., and Jorns, M. S. (2005) Ionization of zwitterionic amine substrates bound to monomeric sarcosine oxidase. *Biochemistry 44*, 16866–16874.
42. Dunn, R. V., Marshall, K. R., Munro, A. W., and Scrutton, N. S. (2008) The pH dependence of kinetic isotope effects in monoamine oxidase A indicates stabilization of the neutral amine in the enzyme-substrate complex. *FEBS J. 275*, 3850–3858.
43. Dansen, T. B., Wirtz, K. W. A., Wanders, R. J. A., and Pap, E. H. W. (1999) Peroxisomes in human fibroblasts have a basic pH. *Nat. Cell Biol. 2*, 51–53.
44. Ralph, E. C., Anderson, M. A., Cleland, W. W., and Fitzpatrick, P. F. (2006) Mechanistic studies of the flavoenzyme tryptophan 2-monooxygenase: Deuterium and ^{15}N kinetic isotope effects on alanine oxidation by an L-amino acid oxidase. *Biochemistry 45*, 15844–15852.
45. Ralph, E. C., Hirschi, J. S., Anderson, M. A., Cleland, W. W., Singleton, D. A., and Fitzpatrick, P. F. (2007) Insights into the mechanism of flavoprotein-catalyzed amine oxidation from nitrogen isotope effects on the reaction of N-methyltryptophan oxidase. *Biochemistry 46*, 7655–7664.
46. Miller, J. R., and Edmondson, D. E. (1999) Structure-activity relationships in the oxidation of para-substituted benzylamine analogues by recombinant human liver monoamine oxidase A. *Biochemistry 38*, 13670–13683.
47. Ghisla, S., and Massey, V. (1991) L-Lactate oxidase. In *Chemistry and Biochemistry of Flavoenzymes* (Muller, F., Ed.) Vol. II, pp 243−289, CRC Press, Boca Raton, FL.
48. Emanuele, J. J., Jr., and Fitzpatrick, P. F. (1995) Mechanistic studies of the flavoprotein tryptophan 2-monooxygenase. 1. Kinetic mechanism. *Biochemistry 34*, 3710–3715.
49. Lee, M. B., Winder, C., Cooch, H., and Shiekhattar, R. (2005) An essential role for CoREST in nucleosomal histone3 lysine4 demethylation. *Nature 437*, 432–435.

BI802227M